Estimating motor unit discharge pattern from the surface electromyogram

Estimating motor unit discharge patterns from high-density surface electromyogram

Aleš Holobar [a,b], Dario Farina [c], Marco Gazzoni [b], Roberto Merletti [b,*], Damjan Zazula [a]

[a] Faculty of Electrical Engineering and Computer Science, University of Maribor, Maribor, Slovenia
[b] Laboratorio di Ingegneria del Sistema Neuromuscolare, Politecnico di Torino, Dipartimento di Elettronica, Corso Duca degli Abruzzi, 24, 10129 Torino, Italy
[c] Center for Sensory–Motor Interaction (SMI), Department of Health Science and Technology, Aalborg University, Aalborg, Denmark

A B S T R A C T

Objective: We systematically tested the capability of the Convolution Kernel Compensation (CKC) method to identify motor unit (MU) discharge patterns from the simulated and experimental surface electromyogram (sEMG) during low-force contractions.
Methods: sEMG was detected with a grid of 13 × 5 electrodes. In simulated signals with 20 dB signal-to-noise ratio, 11 ± 3 out of 63 concurrently active MUs were identified with sensitivity >95% in the estimation of their discharge times. In experimental signals recorded at 0–10% of the maximal force, the discharge patterns of (range) 11–19 MUs (abductor pollicis; n = 8 subjects), 9–17 MUs (biceps brachii; n = 2), 7–11 MUs (upper trapezius; n = 2), and 6–10 MUs (vastus lateralis; n = 2) were identified. In the abductor digiti minimi muscle of one subject, the decomposition results from concurrently recorded sEMG and intramuscular EMG (iEMG) were compared; the two approaches agreed on 98 ± 1% of MU discharges.
Conclusion: It is possible to identify the discharge patterns of several MUs during low-force contractions from high-density sEMG.
Significance: sEMG can be used for the analysis of individual MUs when the application of needles is not desirable or in combination with iEMG to increase the number of sampled MUs.

1. Introduction

Recording of the electrical activities of motor units (MUs) provides an insight into the activation properties of the motoneurons that are located in the spinal cord (De Luca et al., 1982). However, electric signals detected from muscles comprise the contributions of all the MUs which are active within the detection volume of the recording system. Analysis of MU discharges thus requires automated signal decomposition (De Luca and Adam, 1999; McGill and Dorfman, 1985; Stashuk, 2001) which attempts to resolve a composite EMG signal into its constituent MU action potential (MUAP) trains.

Identification of individual MU electrical activities in vivo is classically performed by intramuscular EMG (iEMG), which has high spatial selectivity and thus comprises the contributions of a relatively small number of active MUs whose fibers are close to the recording point (De Luca and Adam, 1999; McGill and Dorfman, 1985; Stashuk, 2001; Nawab et al., 2008). Because this method is invasive, it has limitations in cases when needle insertion is not possible or not desirable, such as in clinical examinations of children, professional athletes, patients with transplanted limbs (Farina et al., 2008a) or haemophilia, and, in general, in dynamic conditions, during work, sport or space activities. Moreover, the identified intramuscular action potentials are not representative of all the fibers in the MU (Stålberg, 1980) and it is not possible to detect the same MUs in repeated measurements. With indwelling EMG recordings, it is also difficult to extract parameters related to the membrane properties of the muscle fibers, such as action potential propagation velocity (Farina et al., 2001; Merletti, 1994), and anatomical characteristics of the MUs, such as fiber length, fiber orientation, and location of the innervation zone (Merletti, 1994). The information on membrane and anatomical fiber properties is relevant in several applications, e.g., for studying muscle fatigue or the effect of location for the injection of substances such as botulin toxin.

* Corresponding author. Tel.: +39 011 4330476; fax: +39 011 4330404.
E-mail address: roberto.merletti@polito.it (R. Merletti).

Global myoelectric activity can also be detected non-invasively by electrodes placed over the skin (Merletti and Parker, 2004). The lower selectivity of surface EMG (sEMG) recordings combined with a larger muscle area covered by non-invasive electrodes with respect to iEMG, may overcome some of the limitations of iEMG, however it makes the decomposition of the signal substantially more challenging. Identification of the complete MU discharge pattern from sEMG can be currently performed mainly in special conditions, such as MU reinnervation (Lanzetta et al., 2005; Farina et al., 2008a) or selective activation through visual feedback (Farina et al., 2004). De Luca et al. (2006) proposed a method for decomposition of four-channel sEMG that showed high accuracy on a few representative recordings. However, the method requires substantial interaction with an expert operator and is theoretically limited by the small information content of a four-channel detection system (Farina et al., 2008b; Merletti et al., 2008b).

There have been substantial efforts in the development of methods for the decomposition of sEMG recorded with high-density electrode grids (Blok et al., 2002; Gazzoni et al., 2004; Kleine et al., 2007; Wood et al., 2001). Farina et al. (2008b) proved by simulations and experimental recordings the necessity of detecting many signals over the skin surface for successful sEMG decomposition. Using multi-channel recordings, Gazzoni et al. (2004) applied the template matching MUAP segmentation and classification technique, and Wood et al. (2001) employed a finite element analysis to investigate the relationship between surface potential distribution and MU depth. Blind source separation techniques (Garcia et al., 2005; Nakamura et al., 2004) and higher-order statistics (Zazula and Holobar, 2005) have also been proposed for MU identification from sEMG. These methods, however, cannot automatically identify the complete MU discharge pattern from sEMG or can identify only a small number of concurrently active MUs.

Recently, Holobar and Zazula (2004, 2007) proposed the Convolution Kernel Compensation (CKC) approach that was proven to provide a good approximation of complete MU discharge patterns in simple test cases, during constant force contractions and with a small number of active MUs. This method is potentially suitable for MU investigations, but is of limited use in practice because a comprehensive analysis of its performance is still lacking. The lack of performance analysis in a variety of conditions is a general issue related to any decomposition algorithm currently available for sEMG. Consequently, the use of sEMG for the analysis of the MU discharge pattern is not yet considered appropriate in physiological and clinical studies.

The purpose of this study was to systematically examine the CKC capability to decompose sEMG recorded during isometric low-level force-varying contractions. In particular, we tested the potential of the CKC method to (1) identify a relatively large sample of MUs from a population of many concurrently active MUs, (2) track early-recruited MUs when higher-threshold MUs are additionally recruited, (3) identify MUs from muscles with different anatomies, (4) identify MUAP trains in agreement with iEMG decomposition. The results provide the first comprehensive performance analysis of a method for sEMG decomposition and validate the use of high-density sEMG for the analysis of individual MUs.

2. Materials and methods

The CKC decomposition method was described by Holobar and Zazula (2007). Because tests on only simulated signals or only experimental signals are not sufficient to assess the accuracy of a decomposition algorithm, in this study results from both signal types are reported. Moreover, the experimental signals have been recorded from muscles with different anatomies to test the sensitivity of the CKC method to differences in the volume conductor properties. The local ethics committee approved all experimental recordings and all the subjects involved signed an informed consent form before participation.

2.1. Simulated signals

The simulations were based on a model of recruitment of a population of MUs (Fuglevand et al., 1993) and a volume conductor model (Farina and Merletti, 2001). The volume conductor was planar with muscle, subcutaneous, and skin tissues. The simulations comprised three main steps: (1) determining the recruitment and discharge times of a population of motor neurons in response to a given level of excitation; (2) generating MUAPs from estimates of the number, location, and conduction velocities of the muscle fiber action potentials for each MU; and (3) simulating the sEMG by summing the trains of MUAPs. The simulation modalities were similar to those previously described by Keenan et al. (2005) but the detection was performed with an electrode grid.

2.1.1. Motor unit action potentials

The volume conductor model was implemented in Matlab (The Mathworks, Natick, MA). The basic parameters for the model were the same as described in Keenan et al. (2005). The distributions of properties across the MU pool were based on the size principle (Henneman, 1957) and included innervation number, recruitment threshold, MU territory, and conduction velocity of MU potentials progressively increasing with the simulated muscle excitation level.

The planar volume conductor consisted of an anisotropic, semi-infinite muscle layer, and isotropic subcutaneous (1.5-mm thick) and skin layer (1-mm thick). A muscle with elliptical cross-section (transversal $\times$ depth, 16 $\times$ 10 mm) was simulated. The number of muscle fibers was 41,000, based on an average fiber diameter of 56 μm (Dennett and Fry, 1988), a muscle cross-section of 100.53 mm^2, and an assumption that the non-contractile tissue accounted for 20% of the cross-sectional area. These values were similar to those used by Keenan et al. (2005).

Each tissue layer was homogeneous and the conductivity properties of each layer were the same as those reported by Farina and Merletti (2001): the subcutaneous and skin tissues were isotropic, whereas the muscle was anisotropic, with conductivity ratio = 5 between the longitudinal and transverse direction. The conductivity ratio was 20 between the skin and subcutaneous layers and 0.5 between the subcutaneous and the muscle (along the transverse direction). Average fiber length was 30 mm and the centers of the innervation zones were located at -3.5 or 7.5 mm (random for each MU) from the center of the detection system. The endplate and insertion of each fiber into the tendons varied randomly (uniform distribution) over a range of 2.5 mm.

The muscle comprised a total of 120 MUs randomly distributed within its cross-section. The fibers of a MU were randomly scattered in a circular MU territory, with a density of 20 fibers/mm^2 (Stålberg and Antoni, 1980; Armstrong et al., 1988), and interdigitated with fibers belonging to many other units to yield a muscle fiber density of 200 fibers/mm^2. When a portion of the MU territory was constrained by the muscle boundary, the territory of the unit was modified to fit the muscle cross-section (Keenan et al., 2005). Innervation numbers were uniformly distributed across the simulated motor units and ranged from 25 to 2500 based on a ~100-fold range of twitch forces (Elek et al., 1992). The MUs had normally distributed conduction velocities with the mean and standard deviation of 4.0 ± 0.3 m/s (Farina et al., 2000) and with the smallest MUs assigned the slowest conduction velocities (Andreassen and Arendt-Nielsen, 1987). The fibers belonging to the same MU had the same conduction velocity. The simulation of the intracellular action potential was based on the analytical description of Rosenfalk (1969).

2.1.2. Discharge pattern

In the simulated 12 s long contractions, the excitation level to the muscle increased from 0% to 10% in the first 6 s and decreased from 10% to 0% in the last 6 s. The distribution of recruitment thresholds for the motor neurons was modelled as described by Fuglevand et al. (1993), with an exponential function with many low-threshold neurons and progressively fewer high-threshold neurons. The number of MUs active at 10% excitation level was 63 out of 120. Each MU discharged at 8 pulses per second (pps) once excitation exceeded the assigned recruitment threshold, and discharge rates increased linearly (0.3 pps/%) with excitation. The peak discharge rate was 35 pps for all the simulated MUs. The last unit was recruited at 50% maximal excitation. Discharge rate variability was modelled as a Gaussian random process with coefficient of variation of the interspike interval equal to 20%.

2.1.3. Detection system

The recording system was a grid of 13 × 5 electrodes of circular shape (radius 1 mm) with 3.5-mm interelectrode distance in both directions. A bipolar recording was simulated for each longitudinal pair of adjacent electrodes, thus leading to 60 simulated detection points. The center of the grid was over the center of the muscle in the longitudinal and transverse direction. The surface-recorded MU potential was the sum of the action potentials of the muscle fibers belonging to the MU. EMG signals were computed at 2048 samples/s. Zero-mean Gaussian noise, with signal-to-noise ratio (SNR) 0–20 dB (5 dB increments) and bandwidth 20–450 Hz was added to the simulated recordings.

2.2. Experimental signals: abductor pollicis brevis

A set of experimental sEMG was recorded from the abductor pollicis brevis muscle of eight healthy men (age, mean ± SD: 27.3 ± 2.2 yr; stature 1.79 ± 0.07 m; body mass 75.2 ± 7.4 kg) in similar conditions as in the simulations.

The sEMG was detected with a two-dimensional grid of 61 silver electrodes (1-mm diameter, 3.5-mm interelectrode distance, 13 rows and 5 columns, without the four corner electrodes) from the abductor pollicis brevis muscle of the dominant hand. The acquired signals were amplified (LISiN-OT Bioelettronica, Torino, Italy), band-pass filtered (3 dB bandwidth, 10–500 Hz), sampled at 1650 samples/s, and converted to digital form by 12-bit A/D converters.

The electrode grid was located with the columns in the direction of the muscle fibers and the last row approximately on the proximal tendon ending. Before electrode placement the skin was abraded with abrasive paste (Meditec–Every, Parma, Italy). The grid was fixed on the skin by adhesive tape and a reference electrode was placed at the wrist.

A custom designed brace was used to measure abduction force. The subject's wrist was fixed in a padded wood support with the head of the thumb phalanx in touch with a load cell (model 8523-50N, Burster, Gernsbach, Germany). The force signal was amplified (Force Amplifier, MISO-II, LISiN, Torino, Italy), provided as feedback to the subject on an oscilloscope, and recorded in parallel with the EMG.

The subjects performed three maximal voluntary contractions (MVCs) separated by 2 min of rest; the highest measured force value corresponded to 100% MVC. The electrode grid was then placed over the abductor pollicis brevis muscle and the subject was asked to linearly increase the force from 0% to 10% MVC in 6 s and then decrease it from 10% to 0% MVC in 6 s, using a visual feedback on force provided on an oscilloscope. Five consecutive repetitions of force ramps were recorded from each subject.

2.3. Experimental signals: biceps brachii, upper trapezius, and vastus lateralis

In order to experimentally test the decomposition method in muscles with different fiber architecture and size, experimental signals were also recorded from the dominant biceps brachii, upper trapezius and vastus lateralis muscles of two healthy men (age 35 and 31 yrs), during isometric variable-force contractions. For these recordings, an adhesive two-dimensional grid of 64 electrodes (SpesMedica, Italy; electrodes with 1-mm diameter, 8-mm interelectrode distance, 13 rows and 5 columns with the first corner electrode missing) was used. In order to cover most of the muscle surface area, a larger interelectrode distance was used for biceps, upper trapezius and vastus lateralis muscles with respect to the abductor pollicis brevis. The signals were acquired with the same EMG amplifier and settings as for the abductor pollicis brevis muscle.

The exerted muscle force was measured by custom made isometric braces (LISiN, Politecnico di Torino, Italy) equipped with load cells (CCT Transducers, Torino, Italy). In the case of the biceps brachii, the subject's arm was fixed in a brace with the upper arm abducted at 90° in the lateral plane and elbow joint angle of 120° (180° = full elbow extension). For the vastus lateralis, the subject was seated with his trunk supported and with arms crossed on the chest. The pelvis was firmly strapped with a velcro belt and the dominant leg was placed in a brace at the knee joint angle of 120° (180° = full knee extension). For the measurements from the upper trapezius muscle, the subject was seated on a chair, with the arms straight alongside the body to reduce the involvement

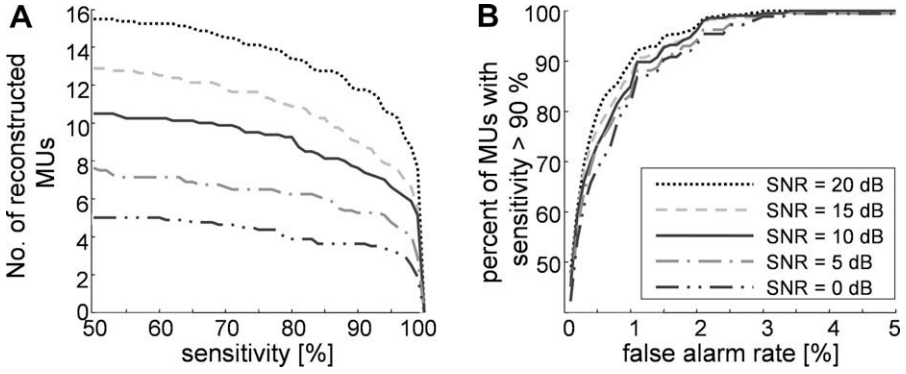

Fig. 1. (A) Cumulative number of MUs reconstructed from simulated sEMG as a function of sensitivity (Eq. (1)). For 20 dB SNR, more than 11 MUs were identified with average sensitivity in detection of MU discharges larger than 95%. (B) Cumulative percentage of identified discharge patterns with sensitivity >90% as a function of the false alarm rate (Eq. (2)). Almost all identified discharge patterns had false alarm rate <2%, whereas for 90% of identified MU discharge patterns the false alarm rates were <1%. Results are averaged over 40 simulations.

of the biceps brachii and deltoid muscles, the back leaned against the back of the chair to avoid the activity of the erector spinae muscles, and the feet raised to avoid contributions from the lower limb muscles. A bilateral pull was performed to avoid trunk bending. Force was measured by two load cells (UU-K200, DACELL, Korea) connected to handles which were pulled up bilaterally by the subject. Force profiles requested to the subjects for the biceps brachii, upper trapezius, and vastus lateralis muscles were identical as those recorded from the abductor pollicis brevis (ramp upwards and downwards at 10% MVC in 12 s in total).

2.4. Experimental signals: concurrent recordings of iEMG and sEMG

In order to provide a direct measure of sensitivity of the decomposition method, an additional experiment was conducted on one healthy man (age 25 yrs) with concurrent recording of sEMG and iEMG signals from the dominant abductor digiti minimi muscle. A grid of surface electrodes (13×5 electrodes, 3.5 mm interelectrode distance) was located between the most distal innervation zone and the distal tendon region of the muscle in the direction of the fibers. Two wire electrodes made of Teflon coated stainless steel (A-M Systems, Carlsborg, WA, USA) were inserted into the muscle with a 25 G needle proximal to the surface grid. The insulated wires were cut to expose only the cross-section at the tip. The needle was inserted to a depth of a few millimeters below the muscle fascia and removed to leave the wire electrodes inside the muscle. A reference electrode for both the surface and intramuscular recordings was placed around the wrist. The sEMG was acquired with the same amplifier and settings as for the abductor pollicis brevis muscle. The iEMG signals were amplified and provided bipolar recordings (Counterpoint EMG, DANTEC Medical, Skovlunde, Denmark) that were band-pass filtered (500 Hz–5 kHz). The fifth finger was fixed in a custom-made brace to record the force exerted during an isometric contraction of the muscle (LISiN, Politecnico di Torino, Torino, Italy). The subjects performed three maximal voluntary contractions with the abductor digiti minimi,

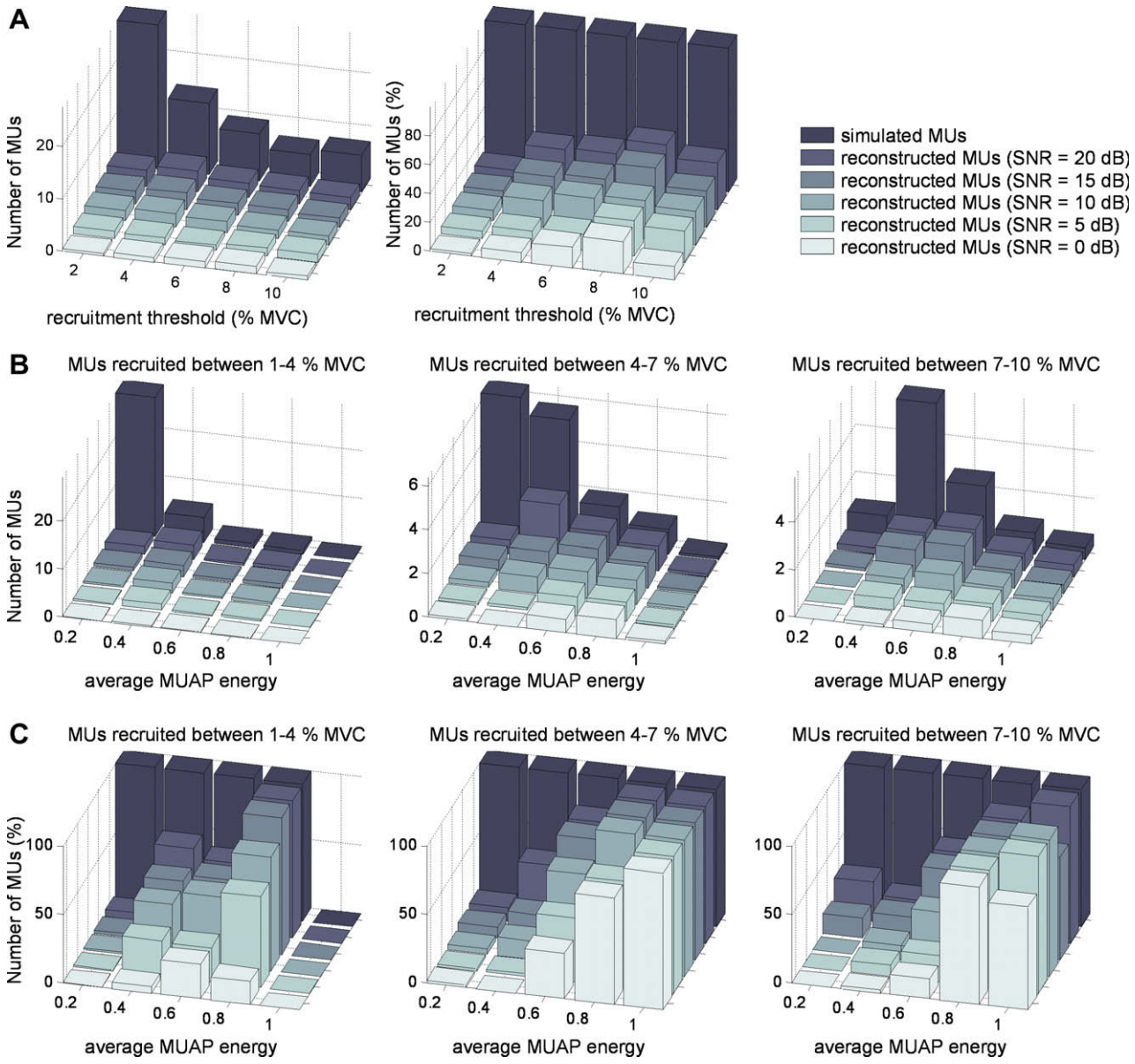

Fig. 2. (A, left panel) Number of MUs identified from simulated sEMG versus their recruitment threshold. (A, right panel): Same data as in the left panel, with the number of identified MUs normalized (%) by the number of simulated MUs. (B) Number of identified MUs versus the normalized energy of their multi-channel surface MUAPs. The energy was computed for each MU as the average energy of the MUAPs over all channels. The normalization was done with respect to the highest average energy over the simulated MUs. (C) Same data as in (B), with the number of identified MUs normalized by the number of simulated MUs. The results are averaged over 40 simulations.

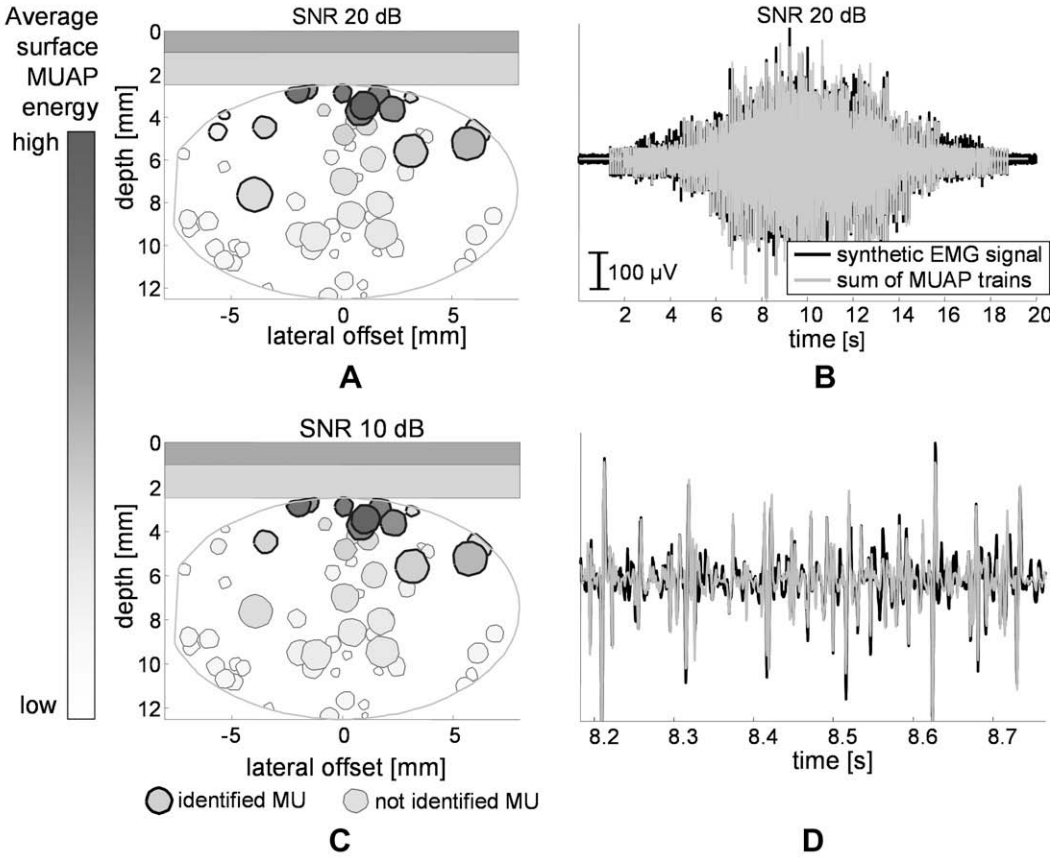

Fig. 3. (A) Simulated MU territories in the muscle tissue and their relative surface MUAP energy for SNR of 20 dB. Identified MUs are encircled with thick black circles, not identified MUs with thin black circles. The intensity of filling represents the average surface MUAP energy. (B) The sum of the identified MUAP trains (*grey line*) compared to the original (simulated) signal (*black line*) for SNR of 20 dB. (C) As in (A) but with 10 dB SNR. (D) A shorter signal segment from the same comparison as in (B).

with each trial separated by 2 min of rest. The greatest force was used as the reference MVC for the submaximal contractions. The subject then performed a 20-s contraction at 10% MVC during which sEMG and iEMG signals were recorded concurrently.

2.5. Signal analysis

Both simulated and experimental signals were decomposed with the CKC method (see Holobar and Zazula (2007) for technical details). For simulated signals, four performance measures were computed: the number of identified MUs, the distribution of their recruitment thresholds, the percentage of correctly identified discharges per MU, i.e. decomposition sensitivity as defined in Eq. (1), and false alarm rate, as defined in Eq. (2):

$$Se_j = \frac{TP_j}{TP_j + FN_j}, \tag{1}$$

$$Fa_j = \frac{FP_j}{FP_j + FN_j}, \tag{2}$$

Table 1
Number of identified MUs, their discharge rates at recruitment, derecruitment, and at the peak force, inter-pulse interval variability, MUAP peak-to-peak amplitude, and conduction velocity identified from sEMG of the abductor pollicis brevis muscle of eight subjects. The discharge rates at recruitment and derecruitment were defined as the average discharge rates of the first and last 5 discharges and the peak discharge rate was defined as the maximum value obtained from the average rate over 5 consecutive discharges. Inter-pulse interval variability was calculated as a coefficient of variation of discharge rate over 1 s long non-overlapping epochs of reconstructed MU discharge patterns. Conduction velocity was estimated with the multi-channel algorithm described by Farina et al. (2001) from double differential derivations. For each reconstructed MUAP template, three channels showing a clear propagation and small shape changes of the potential waveform were selected for conduction velocity estimation. All data are reported as mean ± SD.

Subject	No. of identified MUs	MU discharge rates [pps]			Inter-pulse variability [%]	MUAP amplitude [μV]	Conduction velocity [m/s]
		Recruitment	Force peak	Derecruitment			
A	19	8.4 ± 1.7	14.5 ± 1.9	8.7 ± 1.5	10.6 ± 6.6	166 ± 128	3.8 ± 0.7
B	19	8.6 ± 1.8	18.7 ± 1.8	9.1 ± 1.7	7.6 ± 5.0	242 ± 192	3.4 ± 0.6
C	18	9.1 ± 1.9	16.6 ± 2.5	10.0 ± 1.0	6.6 ± 3.9	192 ± 118	4.2 ± 0.5
D	11	9.8 ± 1.5	17.1 ± 2.0	8.4 ± 2.1	9.0 ± 6.7	170 ± 96	3.4 ± 0.6
E	18	8.8 ± 1.3	15.7 ± 1.9	8.3 ± 1.3	9.0 ± 6.0	144 ± 84	3.8 ± 0.6
F	16	9.8 ± 1.8	17.1 ± 3.8	7.8 ± 1.6	8.4 ± 5.3	118 ± 86	3.6 ± 0.5
G	19	7.7 ± 1.3	13.2 ± 1.5	8.8 ± 1.2	10.2 ± 7.1	98 ± 78	4.3 ± 0.5
H	14	9.7 ± 1.3	14.1 ± 1.1	9.3 ± 1.2	10.0 ± 6.0	162 ± 106	3.3 ± 0.6
Average	17 ± 3	9.0 ± 1.6	15.6 ± 2.1	8.8 ± 1.5	8.9 ± 5.8	161 ± 111	3.7 ± 0.6

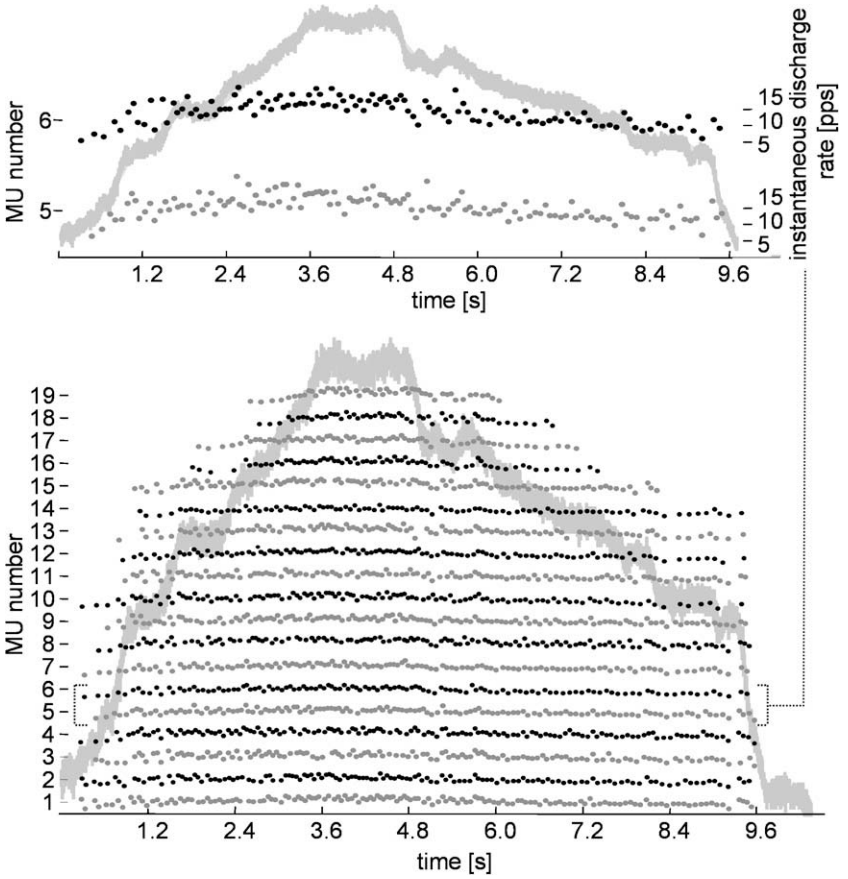

Fig. 4. Instantaneous discharge rate of the MUs identified from abductor pollicis brevis (Subject G). Each dot indicates a MU discharge at a given time instant. The grey line represents the exerted muscle force. The upper panel depicts the details for MUs 5 and 6.

where TP_j (true positives) denotes the number of correctly identified discharges for the jth identified MU, FP_j (false positive) is the number of misplaced discharges and FN_j (false negatives) stands for the number of unidentified discharges. Discharge time tolerance was set equal to ±1 sample. Thus, each identified MU discharge was classified as *TP* if it was detected within ±0.5 ms (sampling rate 2048 samples/s) from its true position along the simulated signal. The values defined in Eqs. (1) and (2) were averaged over the MUs identified in 40 simulations for each SNR value. In each simulation, the locations of the MUs within the muscle tissue were randomly selected.

For experimental sEMG, the following variables were extracted: the number of identified MUs, their recruitment thresholds and their discharge rates at the time of recruitment, derecruitment and at the force peak. The discharge rate at recruitment (derecruitment) was defined as the average discharge rate of the first (last) 5 MU discharges. The peak discharge rate was defined as the average over 5 MU discharges selected around the force peak.

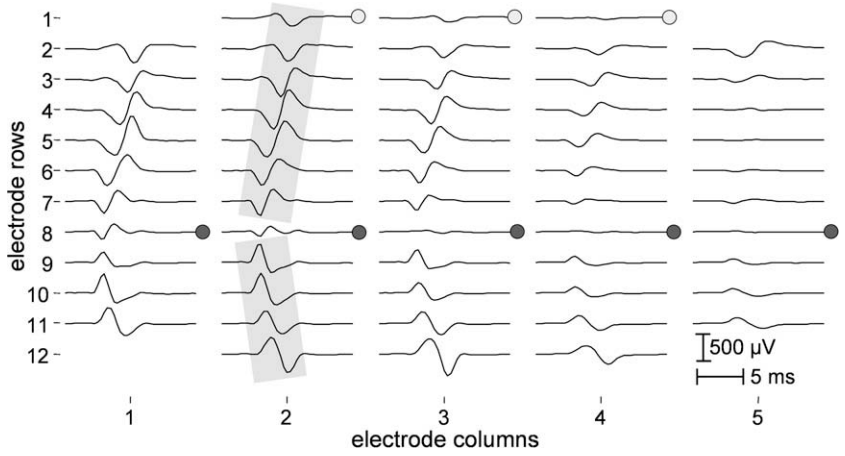

Fig. 5. Multi-channel MUAPs estimated by spike-triggered averaging of sEMG (abductor pollicis brevis, Subject G, MU 6). sEMG were recorded with bipolar derivations with a grid of 61 electrodes arranged in 5 columns and 13 rows (interelectrode distance = 3.5 mm). The location of the innervation zone (*black circles*), tendon regions (*grey circles*) and propagation of MUAPs (*grey rectangles*) are indicated.

The CKC method estimates the MU discharge times, but not the shapes of the action potentials. Thus, the MUAP shapes were estimated by spike-triggered averaging (Keenan et al., 2006) of the sEMG, using the identified MU discharge instants as triggers. The estimated MUAP shapes were convolved with the corresponding MU discharge patterns, summed together, and subtracted from the original sEMG. The following signal-to-interference ratio (SIR) between the original sEMG and the residue after subtraction was then calculated:

$$\mathrm{SIR}(i) = 10 \cdot \log_{10} \frac{E\left[x_i^2(n)\right]}{E\left[\left(x_i(n) - \sum_j z_{ij}(n)\right)^2\right]} \quad (3)$$

where $x_i(n)$ denotes the ith sEMG measurement and $z_{ij}(n)$ stands for the MUAP train of the jth MU reconstructed from the ith sEMG channel.

For the concurrent iEMG and sEMG recordings from the abductor digiti minimi muscle, the iEMG signals were decomposed by the EMGLAB decomposition tool (McGill et al., 2005). Decomposition results were manually inspected, edited by an experienced operator and compared to the automatic results of the CKC-based sEMG decomposition. The percentage of discharges commonly identified at the same time instants by the two decomposition techniques was computed and used as a measure of accuracy, as previously proposed (De Luca et al., 2006). When comparing the decomposition results of the two techniques, discharge time tolerance was set equal to ±0.5 ms, as for the simulated signals.

3. Results

3.1. Simulated signals

Fig. 1 shows the sensitivity and false alarm rates of the reconstructed MU discharge patterns. For 20 dB SNR, 11 ± 3 MUs were identified with average sensitivity in detection of MU discharges larger than 95%. This number decreased with increasing noise power and reached 7 ± 2 MUs for 10 dB SNR. On average, less than 1% of MU discharges were misplaced, even with 0 dB SNR, which proves that the CKC method is highly robust to both noise and action potential superimpositions.

The recruitment thresholds of the identified MUs were approximately uniformly distributed over the entire investigated force range (0–10% MVC) (Fig. 2). For 20 dB SNR, ~16% of the active MUs with recruitment threshold between 1% and 4% MVC were identified. In the same conditions, ~40% of the MUs with recruitment threshold between 4% and 10% MVC were identified (Fig. 2C). The capability to identify MUs depended mainly on the energy of their surface action potentials: almost all MUs with high surface MUAP energy were identified, whereas the MUAPs of deep and small MUs, with low surface energy, were considered a physiological noise by the CKC method (Fig. 2C). All the unidentified MUs with high surface MUAP energy were recruited at levels close to the peak excitation level, thus, they discharged only a few action potentials; because of the small number of discharged action potentials, their activity was considered a signal artefact by the CKC method (Holobar and Zazula, 2004, 2007).

A typical summation of identified MUAP trains is illustrated in Fig. 3 (right panels). Black lines correspond to the simulated sEMG and grey lines to the summation of all identified MUAPs. The SIR, as defined in Eq. (3), was 6.9 ± 1.0 dB (for SNR of 20 dB), 5.7 ± 0.9 dB (15 dB SNR), 4.8 ± 0.8 dB (10 dB SNR), 2.8 ± 0.7 dB (5 dB SNR), and 1.3 ± 0.3 dB (0 dB SNR). Thus, for SNR of 20 dB, the sum of reconstructed MUAP trains accounted for more than 60% of the total sEMG energy. The residue was mainly due to relatively small MUAPs generated by a large number of small and/or deep MUs which were considered noise by the decomposition algorithm (Figs. 2 and 3).

3.2. Experimental signals: abductor pollicis brevis muscle

The discharge patterns of 134 MUs (17 ± 3 MUs per subject; range, 11–19 MUs per contraction) were automatically identified (Table 1). In all subjects, the pool of active MUs was the same over the five consecutive force ramp contractions. Without a reference decomposition result, a direct assessment of the decomposition accuracy was not possible in these recordings. Thus, MU instantaneous discharge rate, inter-pulse interval variability and reconstructed MUAP shapes were examined for consistency with known physiological ranges of values (Table 1). The identified MUs were progressively recruited with increasing contraction force, showing high correlation between the exerted force and the number of identified MUs. Newly recruited MUs began discharging at 9.0 ± 1.6 pps and gradually increased their discharge rate with increasing force (up to 15.6 ± 2.1 pps). Average inter-pulse interval variability was 8.9 ± 5.8% (calculated over 1 s intervals). On the descent side of the ramp, the MU discharge rates decreased to 8.8 ± 1.5 pps and MUs were progressively derecruited in the inverse order with respect to recruitment. The recruitment thresholds of MUs were approximately uniformly distributed over the investigated force range, but this was also significantly influenced by the subject's ability to follow the target force trace (note, for example, the force produced by Subject G in Fig. 4). There was an inverse correlation ($R = -0.37$, $P < 0.0001$) between recruitment threshold and MU peak discharge rate. Reconstructed MU discharge patterns for Subject G are exemplified by the instantaneous discharge rate plot in Fig. 4. Each dot in this plot represents a MU discharge at a given time instant.

Surface MUAP shapes as detected by the electrode grid were estimated by spike-triggered averaging (Keenan et al., 2006) (Fig. 5). As for the simulated signals, the estimated MUAP trains were compared to the original sEMG. The resultant SIR was (average over all subjects) 4.7 ± 1.2 dB. Fig. 6 shows a typical comparison of sum of identified MUAP trains to the original sEMG.

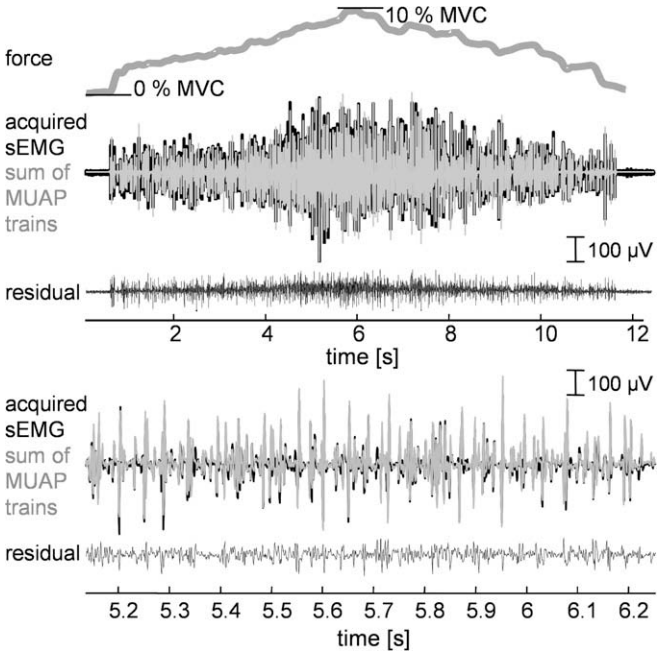

Fig. 6. Sum of identified MUAP trains (grey) compared to the raw sEMG from abductor pollicis brevis (black). The signal acquired by the electrode pair in rows 4–5 of the central grid column is shown, along with the measured thumb abduction force (*top panel*). A shorter portion of the signal is shown in the bottom panel.

3.3. Experimental signals: biceps brachii, upper trapezius and vastus lateralis muscles

The number of MUs identified from the two subjects was 9 and 17 for the biceps brachii, 7 and 11 for the upper trapezius, and 6 and 10 for the vastus lateralis, and remained constant over the consecutive force ramps. MUs were progressively recruited with increasing muscle force and derecruited in inverse order with respect to recruitment. Mean instantaneous discharge rate at the time of MU recruitment was 7.1 ± 1.2 pps (biceps brachii), 7.3 ± 1.9 pps (upper trapezius), and 7.7 ± 1.5 pps (vastus lateralis). At the force peak, MU discharge rates increased to 16.2 ± 2.4 pps (biceps brachii), 21.5 ± 3.8 pps (upper trapezius), and 17.5 ± 2.0 pps (vastus lateralis). Examples of acquired sEMG and identified MU discharge patterns are depicted in Fig. 7.

3.4. Experimental signals: comparison with iEMG decomposition

The discharge patterns of 13 MUs were identified from either sEMG or iEMG of the abductor digiti minimi muscle. Out of 9 MUs identified from sEMG, four were also observed from the iEMG (Fig. 8). In these four commonly identified MUs, the iEMG and sEMG decompositions agreed on 98 ± 1% of the identified MU discharges.

The reconstructed MUAP shapes, as detected by both the central column of the electrode grid and the fine wires, are depicted in Fig. 9B. Commonly identified MUs (surface and intramuscular) contributed with large MUAPs to both the sEMG and iEMG, whereas the MUs identified from the sEMG (iEMG) only, exhibited very low energy in the iEMG (sEMG), as expected. Fig. 9A compares the sum of MUAP trains of 9 MUs identified by CKC to the original sEMG. SIR (averaged over all the sEMG channels) was 7.5 ± 2.0 dB in this recording.

4. Discussion

There have been many attempts to decompose the sEMG (De Luca et al., 2006; Gazzoni et al., 2004; Hogrel, 2003; Holobar and Zazula, 2004; Kleine et al., 2007; Wood et al., 2001). Most methods

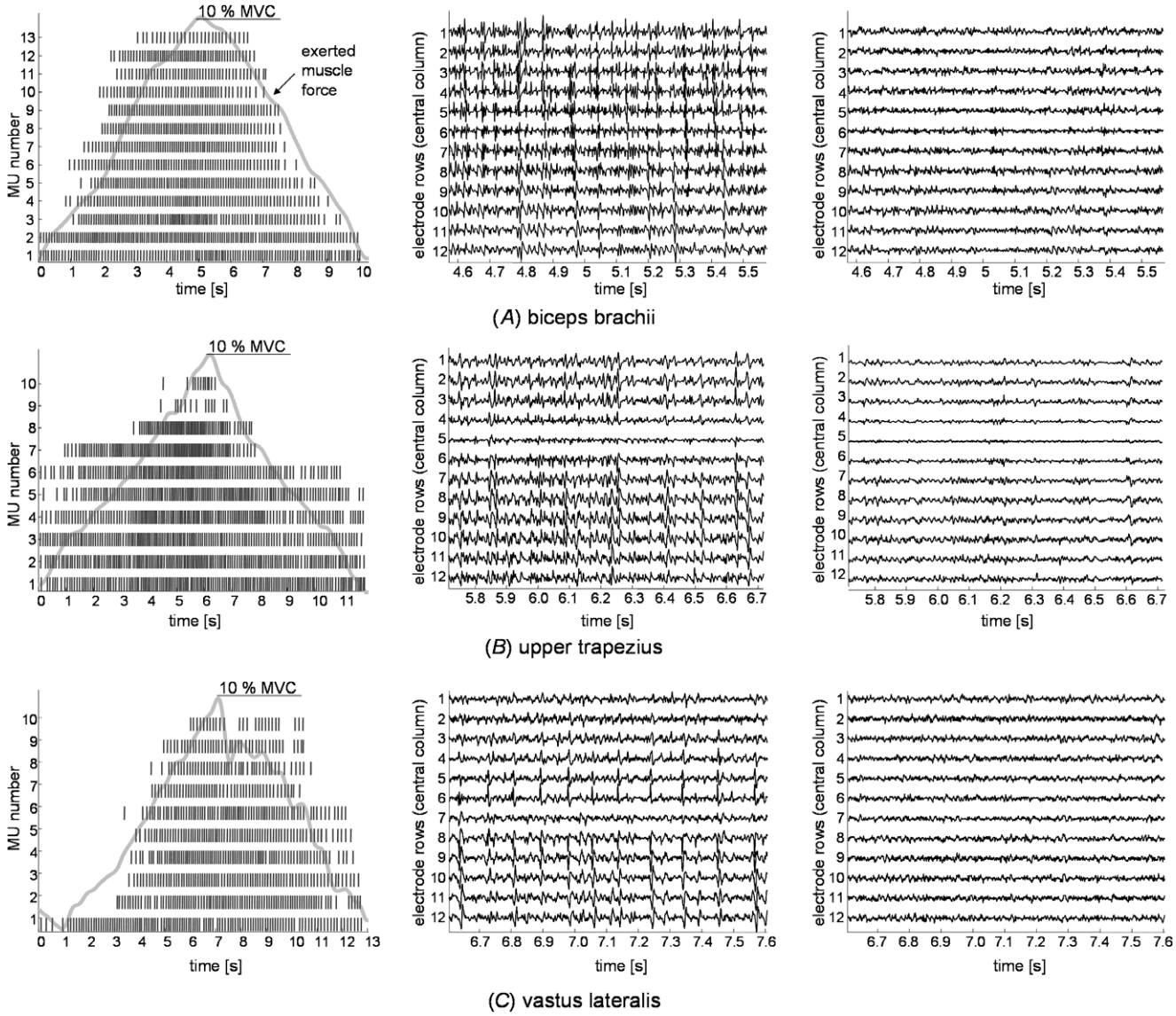

Fig. 7. sEMG recorded by the central column of electrodes (*central panels*), corresponding discharge patterns of identified MUs (*left panels*) and residual after subtraction of identified MUAPs from acquired sEMG (*right panels*) during isometric ramp-up (0–10% MVC) and ramp-down (10–0% MVC) contractions. (A) biceps brachii; (B) upper trapezius; (C) vastus lateralis muscle. Each vertical line indicates a MU discharge at a given time instant. Thick grey line represents the exerted muscle force.

are based on segmentation and classification of MUAPs and require an additional step when superimpositions of action potentials need to be resolved. This approach is feasible in iEMG recordings with limited number of active MUs and relatively high SNR (De Luca, 1993; Doherty and Stashuk, 2003; McGill and Dorfman, 1985). However, it is less convenient for sEMG, especially when the number of concurrently active MUs is large (Merletti, 1994; Stashuk, 2001). An alternative solution is the use of blind source separation methods (Holobar and Zazula, 2004, 2007; Hyvarinen et al., 2001).

Although it has been theoretically demonstrated that the decomposition of the sEMG is feasible when multi-channel recordings are applied (Farina et al., 2008b), the validation of sEMG decomposition algorithms has been limited to a few representative recordings only. Systematic analysis of sEMG decomposition performance is lacking from the literature and consequently there is currently no consensus on the practical suitability of sEMG for investigations of individual MUs. In this study, a method for automatic sEMG decomposition has been tested for the first time on a large set of simulated and experimental signals, so that a quantitative performance analysis could be provided as the basis for the use of sEMG decomposition in physiological and clinical studies.

The classification accuracy obtained in this study is comparable to that obtained by decomposition of intramuscular recordings (De Luca, 1993; McGill and Dorfman, 1985), as also proven by the direct comparison of decomposition results from surface and intramuscular recordings (Fig. 8). The simulations have shown that the CKC method accurately extracts activities of MUs from a rather large muscle area when compared to indwelling EMG (Fig. 3). In experimental sEMG recordings, it was not possible to directly assess the decomposition accuracy. However, estimated average discharge rate, inter-pulse interval variability, and MUAP shapes (peak-to-peak amplitude, innervation zone location, propagation along the fiber direction) were examined for consistency with known physiological range of values (Table 1). For the abductor pollicis brevis muscle, discharge rate at recruitment was on average 7.9 ± 1.6 pps, in agreement with several previous studies (De Luca et al., 1982; Fuglevand et al., 1993; Hogrel, 2003; Søgaard, 1995). The discharge rates at the force peak (10% MVC) were significantly larger than at recruitment and derecruitment and were inversely correlated to recruitment threshold (De Luca et al., 1982; Fuglevand et al., 1993; Hogrel, 2003; Monster and Chan, 1977). For the abductor digiti minimi muscle, the CKC method was directly compared to the decomposition of intramuscular recordings. Comparison of discharge times of four MUs identified by both methods yielded a match of 98%.

The number of MUs detected from the abductor pollicis brevis was on average 17. Although this number was smaller in the biceps brachii, upper trapezius and vastus lateralis muscles, to our knowledge none of the previously proposed sEMG decomposition techniques allows a fully automatic assessment of complete discharge patterns of such a large number of concurrently active MUs. In simulated conditions, the detected MUs were distributed over a large muscle area and thus representative of a large portion of the muscle (Fig. 3). Large superficial MUs were accurately identified, whereas contributions of the deep and/or small MUs were treated as background noise. A limited bias of the CKC method towards the high-threshold MUs was observed, as the early-recruited MUs exhibited lower average MUAP energies than higher-threshold MUs. On average, the identified MUAPs accounted for ~50% of the total signal energy. In experimental conditions, the fraction of signal energy explained by the detected MUAPs ranged from ~40% in the upper trapezius to ~80% in the abductor digiti minimi muscle. The SIR value depends on several intrinsic factors, such as the number of active MUs and the signal quality, which are difficult

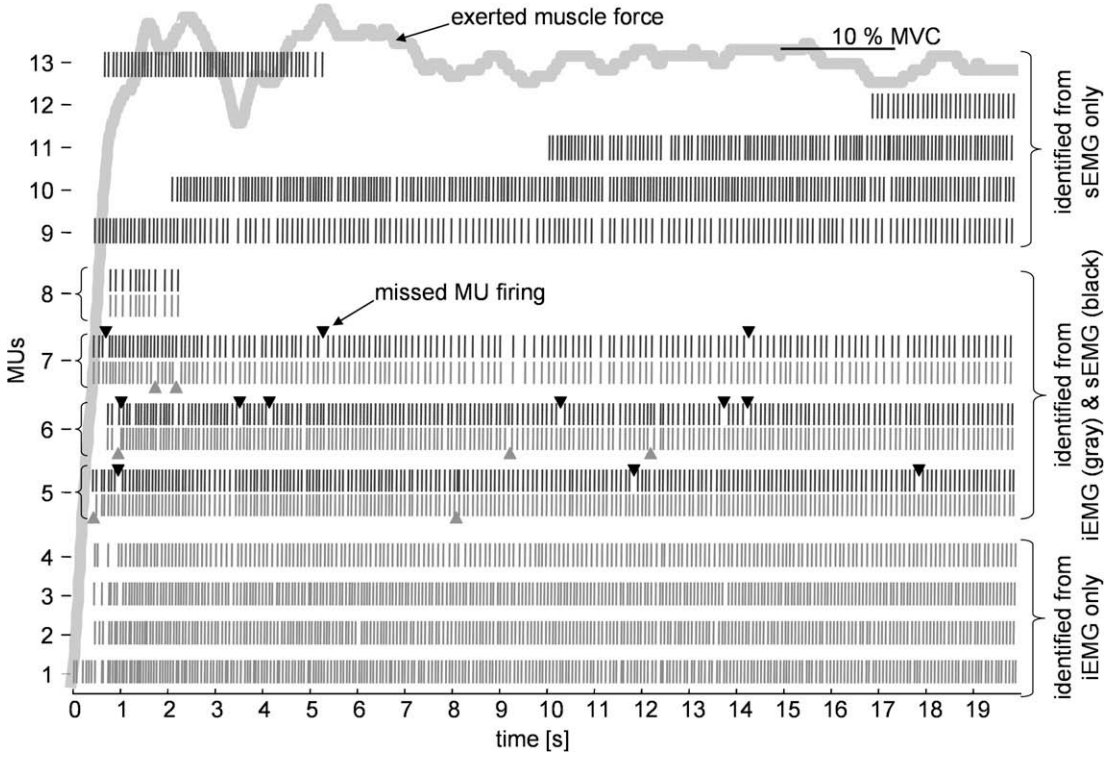

Fig. 8. MU discharge patterns identified by CKC from sEMG (black lines) and by EMGLAB from simultaneously recorded iEMG (grey lines) of the abductor digiti minimi muscle during an isometric constant force contraction at 10% MVC. Each vertical line indicates a MU discharge at a given time instant. MUs 5, 6, 7 and 8 were identified by both CKC and EMGLAB decomposition tools. Their discharge patterns are depicted twice, once as identified by CKC from sEMG (*black*) and once as identified by EMGLAB from iEMG (*grey*). MU discharges, identified by EMGLAB, but not by CKC are denoted with black triangles. MU discharges, identified by CKC, but not by EMGLAB are denoted with grey triangles. The thick grey line represents the exerted muscle force.

to assess in experimental conditions. Nevertheless, in the cases investigated, the residue was due to the activity of MUs with low surface MUAP energies.

Although the number of identified MUs was large when compared to other decomposition methods, the proportion of identified MUs was relatively small when compared to the number of MUs within the detection volume. Thus, generalization of the CKC results to the whole muscle is possible only when MUs with different properties (size, type, etc.) are uniformly distributed within the muscle cross-section so that any region of such cross-section is representative of the rest.

The CKC method is not based on template matching and does not assume predefined MUAP shapes. It only requires the MUAPs to be of limited duration, with shapes relatively constant throughout the contraction. Slow and/or small changes in MUAP shapes (e.g., due to muscle fatigue or moderate muscle shortening against the tendon compliance in isometric force-varying conditions) can be tracked by the algorithm. However, faster changes in MUAP shape may worsen the performance. For example, the action potential propagation velocity depends on the discharge rate (the velocity recovery function of muscle fibers) (Stålberg, 1966) and may substantially vary during the first few discharges therefore affecting MUAP shape. When MUAP shapes change substantially over time, the signal must be divided into shorter stationary epochs that are decomposed independently. In this study, this procedure was not adopted.

MUs with similar MUAP shapes are difficult to discriminate. However, the likelihood that two different MUs have the same sEMG representation decreases with increasing number of recorded channels (Farina et al., 2008b). Out of ~600 synthetic and ~200 experimental MUs identified in this study, only two MUs exhibited MUAPs that could not be distinguished by a grid of 13×5 electrodes (with interelectrode distance of 3.5 mm and 5 mm, respectively) for contraction levels up to 10% MVC. This result is in agreement with the simulation and experimental data by Farina et al. (2008b).

The applied decomposition approach is currently limited to relatively low contraction levels. This limitation is common to all sEMG decomposition techniques and is mainly due to the filtering effect of the subcutaneous tissue, which reduces the morphological differences among MUAPs. The application of the CKC method to signals acquired at higher forces requires the use of more selective spatial filters and larger numbers of acquisition channels (Farina et al., 2008b).

In this study, non-invasive analysis of individual MUs from multi-channel sEMG recordings was validated, justifying the applica-

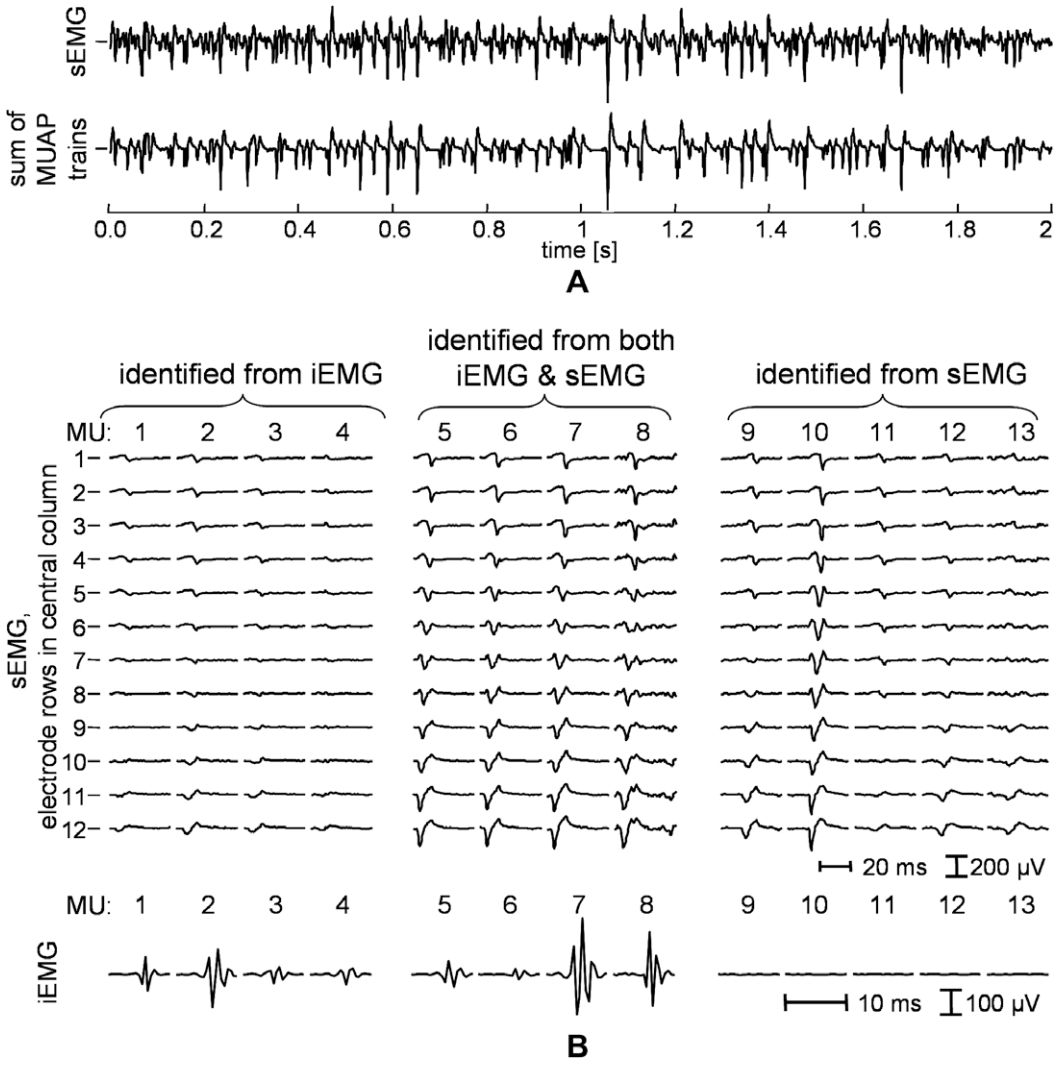

Fig. 9. (A) Sum of identified MUAP trains compared to the sEMG (from the third row of the central column of the grid). sEMG was recorded by a grid of 5×13 electrodes, during an isometric contraction of the abductor digiti minimi muscle at 10% MVC. (B) MUAP templates of 13 MUs, identified either by CKC from sEMG, or by EMGLAB from simultaneously recorded iEMG, and reconstructed by spike-triggered averaging of sEMG channels of the central grid column (*top panel*) and iEMG (*bottom panel*).

tion of the CKC method to physiological studies. The applicability of the CKC method in clinical routine, however, requires further tests of the technique on signals recorded from patients. Pathologies which may be investigated with decomposition of sEMG are those affecting the size and number of MUs, their conduction velocity and their discharge patterns. Beside statistical independence, the CKC method does not assume any other property of the motor unit discharge patterns and can thus be applied in conditions of irregular interspike intervals. However, the condition of independence on the motor unit discharge patterns limits its performance when the degree of motor unit synchronization is high (Holobar and Zazula, 2007).

Although the application of multi-channel detection systems over the skin surface is more time consuming than the use of classic bipolar electrode systems, the current technological solutions for the construction of high-density surface grids include disposable and pre-gelled systems which simplify the mounting procedures (Merletti et al., 2008a,b). Moreover, the CKC decomposition is fully automatic and thus suitable for routine use by inexperienced operators. The computational time depends on the duration of the contraction and complexity of the signal, but in the current version of the method it is acceptable for research investigations. In this study, the CKC method was implemented in Matlab (The Mathworks, Natick, MA) and ran on a PC with a 1.6 GHz CPU and 1 GB memory; under these conditions, the method required ~ 4 min to identify 17 MUs from a 12 s long contraction of the abductor pollicis brevis muscle.

In summary, the CKC decomposition of high-density sEMG allows the identification of the complete discharge pattern of many concurrently active MUs in variable-force contractions and at low force levels. The method was tested in a variety of conditions, including simulated and experimental signals. Although the current study provides confidence in the CKC technique and supports its further use and development, the decomposition of sEMG does not aim at substituting for the classic intramuscular approach, which remains the standard for MU studies; rather, the non-invasive approach may be useful in cases when the use of needles is not possible or not desirable (De Luca et al., 2006), or may be applied together with iEMG to increase the number of identified MUs.

Acknowledgements

This research was supported by a Marie Curie Intra-European Fellowship within the 6th European Community Framework Programme (DE MUSE, Contract No. 023537) (A.H.), by the European project CyberManS (Contract No. 16712) (R.M. and D.F.), by the Danish Technical Research Council (project "Centre for Neuroengineering (CEN)", Contract No. 26-04-0100) (D.F.), by Contract No. C15097/01/NL/SH of the European Space Agency (ESA) on Microgravity effects on skeletal muscles investigated by surface EMG and mechanomyogram, and by Fondazione Cassa di Risparmio di Torino and Compagnia di San Paolo, Torino, Italy (M.G. and R.M.).

References

Andreassen S, Arendt-Nielsen L. Muscle fibre conduction velocity in motor units of the human anterior tibial muscle: a new size principle parameter. J Physiol 1987;391:561–71.

Armstrong JB, Rose PK, Vanner S, Bakker GJ, Richmond FJ. Compartmentalization of motor units in the cat neck muscle, biventer cervicis. J Neurophysiol 1988;60:30–45.

Blok JH, van Dijk JP, Drost G, Zwarts MJ, Stegeman DF. A high-density multichannel surface electromyography system for the characterization of single motor units. Rev Sci Instrum 2002;73:1887–97.

De Luca CJ. Precision decomposition of EMG signals. Methods Clin Neurophysiol 1993;4:1–28.

De Luca CJ, Adam A. Decomposition and analysis of intramuscular electromyographic signals. In: Windhorst U, Heidelberg HJ, editors. Modern techniques. Neuroscience research. Springer; 1999. p. 757–76.

De Luca CJ, Adam A, Wotiz R, Gilmore LD, Nawab SH. Decomposition of surface EMG signals. J Neurophysiol 2006;96:1646–57.

De Luca CJ, LeFever RS, McCue MP, Xenakis AP. Behaviour of human motor units in different muscles during linear-varying contractions. J Physiol 1982;329:113–28.

Dennett X, Fry HJ. Overuse syndrome: a muscle biopsy study. Lancet 1988;331:905–8.

Doherty TJ, Stashuk DW. Decomposition-based quantitative electromyography: methods and initial normative data in five muscles. Muscle Nerve 2003;28:204–11.

Elek JM, Kossev A, Dengler R, Schubert M, Wohlfahrt K, Wolf W. Parameters of human motor unit twitches obtained by intramuscular microstimulation. Neuromuscul Disord 1992;2:261–7.

Farina D, Fortunato E, Merletti R. Noninvasive estimation of motor unit conduction velocity distribution using linear electrode arrays. IEEE Trans Biomed Eng 2000;47:380–8.

Farina D, Gazzoni M, Camelia F. Low-threshold motor unit membrane properties vary with contraction intensity during sustained activation with surface EMG visual feedback. J Appl Physiol 2004;96:1505–15.

Farina D, Merletti R. A novel approach for precise simulation of the EMG signals detected by surface electrodes. IEEE Trans Biomed Eng 2001;48:637–46.

Farina D, Muhammad W, Fortunato E, Meste O, Merletti R, Rix H. Estimation of single motor unit conduction velocity from the surface EMG signal detected with linear electrode arrays. Med Biol Eng Comput 2001;39:225–36.

Farina D, Pozzo M, Lanzetta M, Enoka RM. Discharge variability of motor units in an intrinsic muscle of transplanted hand. J Neurophysiol 2008a;99:2232–40.

Farina D, Negro F, Gazzoni M, Enoka RM. Detecting the unique representation of motor-unit action potentials in the surface electromyogram. J Neurophysiol 2008b;100(3):1223–33.

Fuglevand AJ, Winter DA, Patla AE. Models of recruitment and rate coding organization in motor unit pools. J Neurophysiol 1993;70:2470–88.

Garcia GA, Okuno R, Akazawa K. A decomposition algorithm for surface electrode-array electromyogram. A noninvasive, three-step approach to analyze surface EMG signals. IEEE Eng Med Biol Mag 2005;24(4):63–72.

Gazzoni M, Farina D, Merletti R. A new method for the extraction and classification of single motor unit action potentials from surface EMG signals. J Neurosci Methods 2004;136:165–77.

Henneman E. Relation between size of neurons and their susceptibility to discharge. Science 1957;126:1345–7.

Hogrel JY. Use of surface EMG for studying motor unit recruitment during isometric linear force ramp. J Electromyogr Kinesiol 2003;13:417–23.

Holobar A, Zazula D. Correlation-based decomposition of surface EMG signals at low contraction forces. Med Biol Eng Comput 2004;42:487–96.

Holobar A, Zazula D. Multichannel blind source separation using convolution kernel compensation. IEEE Trans Signal Process 2007;55:4487–96.

Hyvarinen A, Karhunen J, Oja E. Independent component analysis. New York: John Wiley & Sons, Inc.; 2001.

Keenan KG, Farina D, Maluf KS, Merletti R, Enoka RM. Influence of amplitude cancellation on the simulated surface electromyogram. J Appl Physiol 2005;98:120–31.

Keenan KG, Farina D, Merletti R, Enoka RM. Amplitude cancellation reduces the size of motor unit potentials averaged from the surface EMG. J Appl Physiol 2006;100:1928–37.

Kleine BU, van Dijk JP, Lapatki BG, Zwarts MJ, Stegman DF. Using two-dimensional spatial information in decomposition of surface EMG signals. J Electromyogr Kinesiol 2007;17(5):535–48.

Lanzetta M, Pozzo M, Bottin A, Merletti R, Farina D. Reinnervation of motor units in intrinsic muscles of a transplanted hand. Neurosci Lett 2005;373:138–43.

McGill KC, Dorfman LJ. Automatic decomposition electromyography (ADEMG): validation normative data in brachial biceps. Electroencephalogr Clin Neurophysiol 1985;61:453–61.

McGill KC, Lateva ZC, Marateb HR. EMGLAB: an interactive EMG decomposition program. J Neurosci Methods 2005;149:121–33.

Merletti R. Surface electromyography: possibilities and limitations. J Rehabil Sci 1994;7:25–34.

Merletti R, Botter A, Troiano A, Merlo E, Minetto MA. Technology and instrumentation for detection and conditioning of the surface electromyographic signal: state of the art. Clin Biomech 2008a. doi:10.1016/clinbiomech.2008.08.006.

Merletti R, Holobar A, Farina D. Analysis of motor units with high-density surface electromyography. J Electromyogr Kinesiol 2008b;18:879–90.

Merletti R, Parker PA. Electromyography: physiology, engineering, and non-invasive applications. IEEE Press and John Wiley & Sons; 2004.

Monster AW, Chan H. Isometric force production by motor units of extensor digitorum communis muscle in man. J Neurophysiol 1977;40:1432–43.

Nakamura H, Yoshida M, Kotani M, Akazawa K, Moritani T. The application of independent component analysis to the multi-channel surface electromyographic signals for separation of motor unit action potential trains: part I-measuring techniques. J Electromyogr Kinesiol 2004;14(4):423–32.

Nawab H, Wotiz R, De Luca C. Decomposition of indwelling EMG signals. J Appl Physiol 2008;105:700–10.

Rosenfalk P. Intra- and extracellular potential fields of active nerve and muscle fibers. Acta Physiol Scand Suppl 1969;47:239–46.

Søgaard K. Motor unit recruitment pattern during low-level static and dynamic contractions. Muscle Nerve 1995;18:292–300.

Stålberg EV. Propagation velocity in human muscle fibers in situ. Acta Physiol Scand 1966;287:1–112.
Stålberg EV. Macro EMG, a new recoding technique. J Neurol Neurosurg Psychiatry 1980;43:475–82.
Stålberg E, Antoni L. Electrophysiological cross section of the motor unit. J Neurol Neurosurg Psychiatry 1980;43:469–74.
Stashuk DW. EMG signal decomposition: how can it be accomplished and used? J Electromyogr Kinesiol 2001;11:151–73.
Wood SM, Jarratt JA, Barker AT, Brown BH. Surface electromyography using electrode arrays: a study of motor neuron diseases. Muscle Nerve 2001;24:223–30.
Zazula D, Holobar A. An approach to surface EMG decomposition based on higher-order cumulants. Comput Methods Programs Biomed 2005;80:S51–60.